Three-Dimensional Confinement-Related Size Changes to Mixed-Surfactant Vesicles

Ashish K. Jha,[†] Jinkee Lee,[‡] Anubhav Tripathi,*[,‡] and Arijit Bose*[,†]

Department of Chemical Engineering, University of Rhode Island, Kingston, Rhode Island 02881, and Biochemical Engineering Laboratory, Division of Engineering, Brown University, Providence, Rhode Island 02912

Received December 24, 2007. Revised Manuscript Received March 10, 2008

The effect of three-dimensional confinement on the size and morphology of a vesicular surfactant mesophase obtained by mixing micellar solutions of cetyltrimethylammonium bromide and dodecylbenzenesulfonic acid has been studied using small-angle neutron scattering (SANS). The confined spaces were generated by the random close packing of polystyrene beads of radius $R_b = 1.5$, 0.25, and 0.1 μm, creating voids of characteristic dimensions $R \sim 0.22\ R_b = 3300$, 550, and 220 Å, respectively. These void length scales were comparable to or less than the radii of vesicles formed in the system under conditions of no confinement. Vesicles, made by mixing 0.8 wt % micellar solutions of surfactant in a water/D_2O mixture that is contrast-matched with the polystyrene beads, were added in a SANS scattering cell without beads, as well as three cells with the different sized beads. The SANS data from the sample without confinement was best fitted by a core–shell model and not by spheres or disks, confirming the presence of vesicles. The data from samples in the confined domains also showed vesicles as the dominant structure. The most important result is that the mean size of these vesicles decreases as the confinement length scale is reduced. A simple thermodynamic model accounting for the balance between increased enthalpy when vesicles with curvature higher than the preferred one are formed, and increased free volume entropy for smaller vesicles supports the experimental data. While these results are focused on a specific vesicle system, the broad principles behind changes in microstructure produced by confinement are applicable to other surfactant aggregates. The results of this study are potentially important for understanding the flow of drug delivery vehicles through microcapillaries, in the recovery of oil from fine pores in rocks using surfactant containing fluids, micellar enhanced ultrafiltration, or in other situations where the size of surfactant aggregate structures approach the length scales between confining walls.

1. Introduction

Surfactants have an ability to self-assemble into a wide variety of supramolecular structures such as micelles, bilayers, vesicles, and liquid crystals[1] in bulk solution. The lyophobe chain length, nature of solvent, surfactant concentration, temperature, salt concentration, and the presence of one or more cosurfactants[2–4] directly affect supramolecular morphologies. The role of each of these factors is now well studied for bulk systems, that is, where the container dimensions are orders of magnitude larger than the size of the aggregates. In a constrained environment, the length scales characteristic of the confinement geometry can approach the dimensions of the surfactant aggregate structures. In such environments, changes in free volume entropy can have a strong impact on the morphology of evolving structures, potentially making them different from the morphologies observed in bulk systems. These situations are still unexplored and may have applications in the flow of drug delivery vehicles through microcapillaries, oil recovery from fine pores in rocks using surfactant containing fluids, micellar-enhanced ultrafiltration, and detergent applications where soap solutions are required to flow into fabric pores. In thin polymer films, the entropic constraints provided by the presence of boundaries create compositional anisotropy with consequences on morphology and the glass transition temperature.[5] Highly anomalous behavior such as attraction between charged colloids and similarly charged bounding surfaces in confined domains has also been predicted and observed.[6–12]

In this work, we examine the microstructures formed when a vesicle suspension formed by mixing 0.8 wt % cetyltrimethylammonium bromide (CTAB) and 0.8 wt % dodecylbenzenesulfonic acid (HDBS) are placed in an "unconfined" region and in confined three-dimensional geometries created in the spaces between randomly close-packed polystyrene beads. The void size, which can be estimated to be 0.22 times the bead size, is thus varied from orders of magnitude higher (in the experiments without beads) to just a few multiples of the "unconfined" surfactant aggregate size by varying the dimensions of the beads. Changes to the free volume fraction upon confinement introduce entropic effects that can help mitigate enthalpy increases caused by forming "nonbulk" structures, providing a potential thermodynamic pathway for forming morphologies in confined domains that may not be observed in bulk systems. Section 2 describes experimental details; section 3 describes the key results of this investigation.

* Corresponding authors: Arijit Bose, tel 401-874-2804, e-mail bosea@egr.uri.edu; Anubhav Tripathi, tel 401-863-3063, e-mail, Anubhav_Tripathi@brown.edu.

[†] University of Rhode Island.

[‡] Brown University.

(1) Imae, T. *Colloids Surf., A* **1996**, *109*, 291–304.

(2) Koehler, R. D.; Raghavan, S.; Kaler, E. W. *J. Phys. Chem. B* **2000**, *104*, 11035–11044.

(3) Kumar, S.; Aswal, V. K.; Goyal, P. S.; Din, K. *J. Chem. Soc., Faraday Trans.* **1998**, *94*, 761–764.

(4) Freeman, K. S.; Tan, N. C.; Trevino, S. F.; Kline, S.; McGown, L. B.; Kiserow, D. J. *Langmuir* **2001**, *17*, 3912–3916.

(5) Kraus, J.; Müller-Buschbaum, P.; Kuhlmann, T.; Schubert, D. W.; Stamm, M. *Europhys. Lett.* **2000**, *49*, 210–216.

(6) Sader, J. E.; Chan, D. Y. C. *Langmuir* **2000**, *16*, 324–331.

(7) Lowen, H. A., E.; D'Amico, I. *Prog. Colloid Polym. Sci.* **2000**, *115*, 367–370.

(8) Terao, T.; Nakayama, T. *J. Phys.: Condens. Matter* **2000**, *12*, 5169–5177.

(9) Kepler, G. M.; Fraden, S. *Phys. Rev. Lett.* **1994**, *73*, 356–359.

(10) Crocker, J. C.; Grier, D. G. *Phys. Rev. Lett.* **1996**, *77*, 1897–1900.

(11) Larsen, A. E.; Grier, D. G. *Nature (London)* **1997**, *385*, 230–233.

(12) Esselink, F. J.; Semenov, A. N.; ten Brinke, G.; Hadziioannou, G.; Oostergetel, G. T. *Macromolecules* **1995**, *28*, 3479–3481.

10.1021/la704023s CCC: $40.75
Published on Web 05/16/2008

2. Experiments

2.1. Materials. The cationic surfactant CTAB (99% pure) was obtained from Sigma Aldrich and anionic surfactant HDBS from Stepan Company. Deuterium oxide (99.9%) was purchased from Cambridge Isotopes Laboratory. Polystyrene beads of radii 1.5, 0.25, and 0.1 μm were purchased from Duke Scientific Corporation, in the form of a liquid suspension containing 10 wt % solids. The beads were washed three times with deionized water, spread out, and dried at 25 °C for 12 h before being packed into scattering cells used in the experiments.

2.2. Sample Preparation. *2.2.1. Contrast Match of Solvent with Polystyrene Beads.* In order to focus on scattering from the surfactant aggregates only, the scattering length densities from the solvent and the beads were matched. A mixture of H_2O (71.5 mol %) and D_2O (28.5 mol %) created a solvent scattering length density (SLD) equal to that of polystyrene (SLD polystyrene $= 1.41 \times 10^{-6}$ Å^{-2}). This mixture was used as a contrast matched (CM) solvent, thereby making the beads invisible to the incident neutrons. Experiments with slurries of beads in CM solvent produced featureless low-intensity profiles, confirming the quality of the contrast matching (data shown in Supporting Information).

2.2.2. Sample Preparation. Micellar solutions of 0.8 wt % CTAB and 0.8 wt % HDBS were prepared in the CM solvent, and equal volumes of the two micellar solutions were then added to make vesicle solutions. The length between the two quartz faces of the sample-containing cell was 1 mm. Since this length scale is orders of magnitude higher than the largest aggregate structures that are known to form in this system, experiments conducted in scattering cells without beads are assumed to mimic "bulk" behavior. For the experiment with each set of beads, 20 mL of the vesicle solution was mixed with 0.18 g of beads to create a suspension. The suspension was sonicated for 1 h to break up any macroscopic lumps of beads and subsequently degassed for 1 min to remove air voids. The scattering cells were then filled with the suspension and centrifuged (Eppendorf 5810R, Eppendorf Inc.) at 3000 rpm for 10 min to force the beads to pack into the cells.[13] The excess solution on the top of the beads was withdrawn; the cells were replenished with the slurries and centrifuged. This process was repeated until the cells were fully packed with the beads, with the surfactant solution filling the void spaces. The samples were equilibrated at 25 °C prior to data collection.

2.3. SANS Measurements. The SANS measurements were carried out on the 30 m NG7 spectrometer[14] at the NIST National Center for Neutron Research (NCNR, Gaithersburg, MD). The scattered intensity, I, was recorded as a function of the magnitude of the scattering vector q ($q = 4\pi \sin(\theta/2)/\lambda$, where θ is the scattering angle and λ is the neutron wavelength, 6 ± 0.9 Å). Three sample-to-detector distances were used to cover a q-range of 0.003–0.3 Å^{-1}. The raw data were corrected for empty cell scattering, detector sensitivity, background, and transmission through the samples. They were circularly averaged and placed on an absolute scale using software provided by NCNR.

2.4. Surfactant Adsorption Measurements. Given the possibility that some of the surfactants can adsorb on to the surface of the polystyrene beads and hence contribute to the scattering, detailed experiments were carried out to quantify this effect. Vesicle solutions with total surfactant concentrations of 0.8, 0.6, and 0.5 wt % were prepared in deionized water and equilibrated at 25 °C. Absorption at a wavelength of 2880 Å was used to calibrate for concentrations. Three milliliters of 0.8 wt % vesicle solution was added to 0.005 g of 0.1 μm radius polystyrene beads and equilibrated for 24 h. The sample was then centrifuged at 12000 rpm for 5 min, and the absorbance of the supernatant samples at 25 °C was then measured on a UV–vis spectrometer. These data along with the calibrated absorption curve were used to determine the amount of surfactant absorbed on the beads. The 0.1 μm beads provide the largest surface area/mass and therefore represent the most extreme scenario for adsorption.

3. Results and Discussion

The key result of this study is that vesicles of decreasing size are formed as the confinement length scale is decreased. In the discussion below, we present a detailed analysis of the experimental data that leads to this conclusion. We also provide a simple first-order thermodynamic model that accounts for contributions to the Gibbs free energy change because of enthalpy variation caused by changes in vesicle size and free volume entropy effects that shows a reasonable match to the experimental observation.

We first investigate the surfactant aggregate structure in the unconfined domain. The intensity of scattering from a particle assembly can be expressed as[15]

$$I(q) = N_s P(q) S(q) \tag{1}$$

where N_s is the number of scattering centers, $P(q)$ is the intraparticle form factor, and $S(q)$ is the structure factor accounting for interparticle interactions. A core–shell model[15] describing the vesicle geometry is chosen for the form factor, $P(q)$. The vesicle inner radius, bilayer thickness, SLD contrast between the shell and the solvent, and the vesicle volume fraction are the model parameters. SLD contrast is known and provided as input to the least-squares routine used to find the fitting parameters. The form factor is averaged over a Schultz distribution characterized by a mean radius and polydispersity.[16] The average intervesicle distance is $\sim N_v^{-1/3}$, where N_v is the vesicle number density (N_v = vesicle volume fraction/volume of one vesicle). With vesicle radii obtained from cryo-TEM images of ~1000 Å, and using an estimated vesicle volume fraction of ~0.1, the average intervesicle distance is ~3000 Å. (Subsequent fits through the data show ~0.1 to be a good estimate.) Since this distance is comparable to the vesicle size, we allowed the possibility of intervesicle interactions in the scattering data using a Percus–Yevick model for hard spheres for the structure factor.[17] The fit through these data resulted in the "best" values of mean vesicle radius, polydispersity, and the vesicle wall thickness. (We attempted to fit these data using form factors for micelles and disks and found parameters in each case that are not physically realistic. The slope of –2 on a $\log(I)-\log(q)$ plot also indicates the presence of vesicles.)

Figure 1a shows a fit to the scattering data for the unconfined case (no beads). A mean core radius of 969.5 ± 17.3 Å, polydispersity of 0.22 ± 0.01, and bilayer thickness of 30 ± 3.0 Å are obtained from the fit. The bilayer thickness is smaller than twice the length of fully extended CTAB molecule (~30 Å) suggesting that the surfactant molecules are interdigitated within the bilayer. The bilayer thickness is kept fixed at this value for the fitting of SANS data from the remaining experiments.

For each bead size, a set of experiments was conducted where only D_2O (no surfactant) is used to fill the void spaces and used to experimentally determine the volume fraction of spheres in the cell. Our results for these experiments (shown in Supporting Information) are volume fractions of 0.57, 0.73, and 0.65 for 1.5, 0.25, and 0.1μm beads, respectively. The expected volume fraction for random close packing of spheres of ~0.64, and therefore the maximum uncertainty associated in this number, is up to 15%

(13) Alonso, M.; Sainz, E.; Lopez, F. A.; Shinohara, K. *Chem. Eng. Sci.* **1995**, *50*, 1983–1988.
(14) Glinka, C. J.; Barker, J.; Hammouda, B.; Krueger, S.; Moyer, J.; Orts, W. *J. Appl. Crystallogr.* **1998**, *31*, 430–445.
(15) Guinier, A.; Fournet, G. *Small Angle Scattering of X-rays*; Wiley: New York, 1955.
(16) Lee, J. H.; Gustin, J. P.; Chen, T. H.; Payne, G. F.; Raghavan, S. R. *Langmuir* **2005**, *21*, 26–33.
(17) Percus, J. K.; Yevick, G. J. *Phys. Rev.* **1958**, *110*, 1–13.

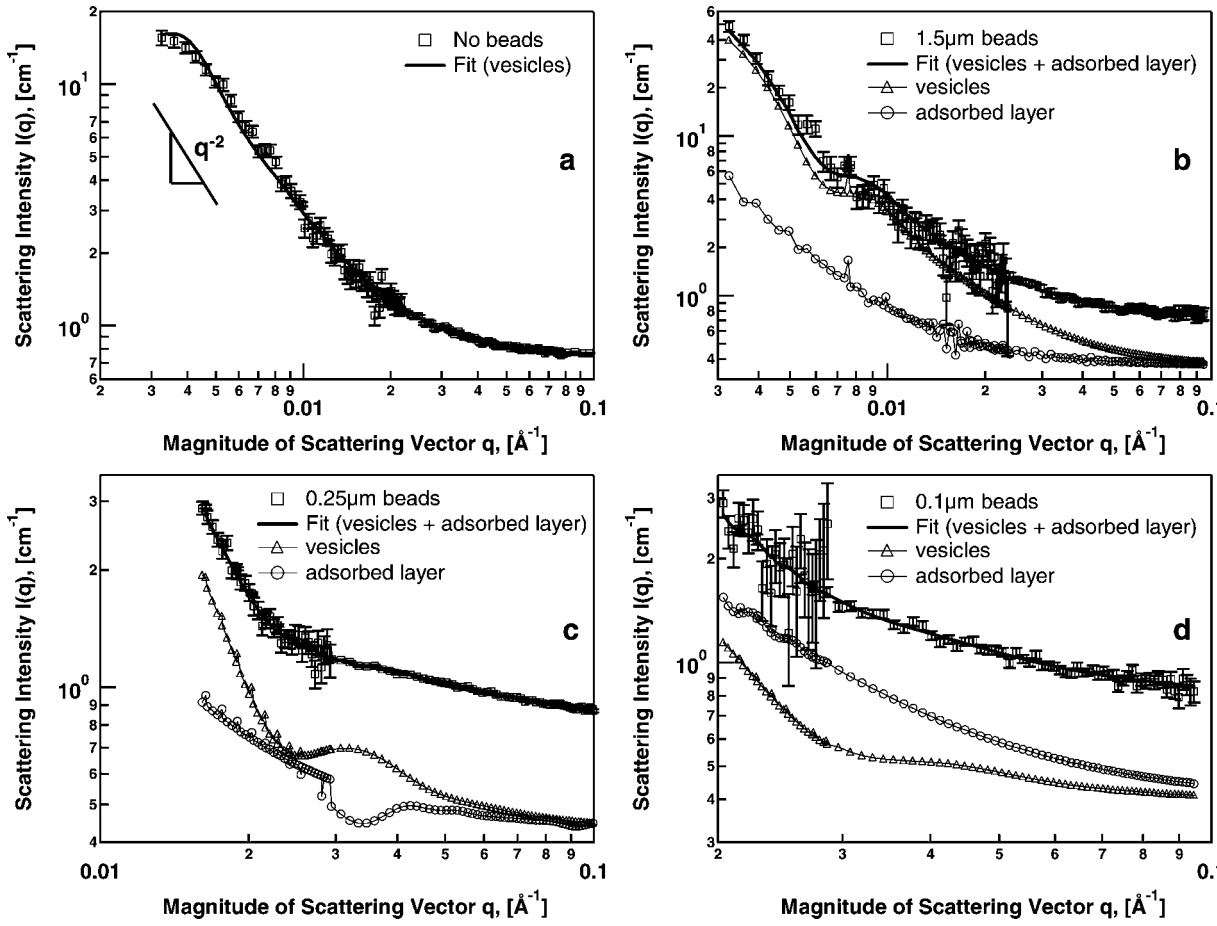

Figure 1. The best fit to the SANS data for the unconfined surfactant sample (a), confined surfactant samples with beads of radius 1.5 μm and void length scale 3300 Å (b), 0.25 μm and void length scale 550 Å (c), and 0.1 μm and void length scale 220 Å (d). Individual contributions to the overall scattering from the adsorbed layer and the suspension in the void spaces are also shown for each of the bead sizes. The fits incorporate a polydispersed vesicle model for the surfactant microstructure and a core–shell model for the surfactant layer adsorbed on the beads.

in our experiments. We have used the SANS data fitting routine to examine the role of uncertainty in bead packing fraction on the radius of the vesicles. For the smallest beads, an uncertainty of 15% in the packing fraction causes an 8% uncertainty in the prediction of vesicle radius under confinement. For bead sizes of 0.25 μm and 1.5 μm, a 15% uncertainty changes the vesicle radius by only 2%. Since each attempt at packing the cell can produce slightly different packing fractions and to avoid additional floating parameters, we chose a fixed bead volume fraction of 0.64 in our data fits.

3.1. Surfactant Adsorption Effects on Concentration. The adsorption measurements give 1.29×10^{-4} mol of surfactant/g of beads for the 0.1 μm radius beads. This implies that 2.3×10^{-5} mol surfactant adsorb on to the beads out of 4.5×10^{-4} mol available in the 20 mL solution in which the beads are suspended. If we assume that the surface characteristics of the other beads are similar, the amount of surfactant adsorbed on the 0.25 and 1.5 μm beads will be, 1.1×10^{-5} and 1.5×10^{-6} mol, respectively, again out of 4.5×10^{-4} mol available in the solution. Adsorption therefore produces negligible reductions of the total surfactant amounts in the void spaces. In order to asses the impact of potential preferential adsorption of one of the surfactants, we calculate the ratio of each surfactant remaining in the solution using an extreme scenario of 10 times greater adsorption of CTAB than HDBS on to the beads. For 0.18 g of 0.1 μm beads in 20 mL of the vesicle solution, the mass ratio of HDBS to CTAB in the solution will then be 1.09:1.0, close to the original ratio of 1:1. Given the low amount of total surfactant adsorption relative to the overall surfactant present in the solution, this result is expected. The reduced specific surface area for the larger beads will mean even lower change to the relative amounts of each surfactant in the void regions. Therefore any preferential adsorption will have negligible impact on the concentration of surfactant in the void regions.

3.2. Scattering from Surfactants in Confined Systems. Given the fact that the solvent is contrast matched with polystyrene beads, any adsorption of surfactants on the beads will contribute to the scattering. For fitting the scattering profiles, we have used a sum model that assumes a core–shell structure for adsorbed surfactants and different plausible structures (see discussion below—polydispersed vesicles ended up being the only reasonable ones) for surfactant microstructures within the void regions. This linear summation of scattering from the adsorbed layers and that from the structures in the void spaces is strictly only valid in a "dilute" regime with no interaction between the adsorbed surfactants and the void space objects. This is assumed in the analysis. The parameters of the core–shell model for the adsorbed surfactant layer are fixed at a volume fraction of 0.64, inner radius equal to the bead radius, and scattering length density of the surfactant at 1.26×10^{-7} Å^{-2} corresponding to a 16-carbon alkane. The thickness of the adsorbed layer is allowed to float for the fit.

Although we have carefully accounted for scattering from the adsorbed surfactant layer, we minimized its impact on the model parameters that defined the objects in the void spaces by focusing on appropriate q ranges during the data fits. For 0.1 μm beads,

Table 1. Vesicle Parameters Obtained by the Fitting of SANS Intensity Profiles

sample	core radius (Å)	core polydispersity
no beads	969.5 ± 17.3	0.22 ± 0.01
1.5 μm beads	446.5 ± 13.4	0.22 ± 0.02
0.25 μm beads	106.5 ± 2.0	0.22 ± 0.02
0.1 μm beads	74.8 ± 4.0	0.28 ± 0.01

the maximum impact from the adsorbed layer is expected at $q \sim 2\pi/L = 0.003$ Å^{-1}, and the data are analyzed for 0.02 Å^{-1} < q < 0.1 Å^{-1}. Similarly for 0.25 μm beads, the maximum impact is expected at $q \sim 2\pi/L = 0.001$ Å^{-1}, and the data are analyzed for 0.015 Å^{-1} < q < 0.1 Å^{-1}. For 1.5 μm radius beads, the maximum scattering is expected at $q \sim 2\pi/L = 0.0002$ Å^{-1}; the considered q-range is 0.003–0.1 Å^{-1}.

Although vesicles are shown to form in the experiments with no confinement, there is no a priori information regarding the structures of the surfactant aggregates in the experiments with beads. Therefore several different models are examined for the surfactant structures, including micelles, disks, and vesicles.[18] The criterion for rejecting or accepting a model is based on the quality of fit as well as how realistic the fitted parameters are. For example, if we assume that the structures in the void spaces created by the 0.1 μm beads are micelles, the best fit produced a micelle size of ~90 Å and a polydispersity of 0.99. Given that CTAB, the longer of the two surfactants used in this study, has a hydrocarbon tail length of ~30 Å, a micelle of 90 Å and a size polydispersity as high as 0.99 are unrealistic. Such unrealistic parameters for micelles size are also predicted for the experiments with the other beads. Thus the micelle model is rejected for this case. For the 0.1 μm beads, a model assuming flat disks produced a disk radius of ~8770 Å, much bigger than the void dimension (~220 Å), again an unrealistic value.[15] A systematic analysis of all the experimental results in this manner showed that the only model for the surfactant aggregates which fitted the data with realistic parameters is one where vesicles are assumed to form.

For the polydispersed vesicle model used to describe the objects in the void spaces, the scattering length densities (SLD) of the CM solvent and the core are assumed equal at 1.41×10^{-6} Å^{-2}. The SLD of the surfactant bilayers are fixed at 1.26×10^{-7} Å^{-2} (coming from the computed SLD of a 16 carbon chain aliphatic layer) while the bilayer thickness is kept fixed at 30 Å. The volume fractions of vesicles, their inner radii, and polydispersities are allowed to float. Panels b−d of Figure 1 show the best fits obtained for the SANS intensity profiles from the structures in the voids of radii 3300, 550, and 220 Å, respectively. The contributions to the overall scattering from the adsorbed layer and the suspension in the void spaces are also shown in panels b−d of Figure 1 (note: the adsorbed layer thicknesses obtained from the fits are 18.9, 12.5, and 16.4 Å for 1.5, 0.25, and 0.1 μm beads, respectively). In the q range of interest, the scattering from the structures in the voids is comparable to that from the adsorbed surfactant layers for all the bead sizes. The important fitting parameters are shown in Table 1. From the volume fraction and dimensions of the vesicles, and using the density of surfactant layer as 0.77 g/cm^3 corresponding to a 16 carbon aliphatic hydrocarbon liquid, the mass fractions of surfactant are 0.0072 ± 0.0008, 0.0076 ± 0.0004, and 0.007 ± 0.0005 for the 1.5, 0.25, and 0.1 μm beads, respectively, which compares well to a mass fraction of surfactant of 0.008 in the original solution.

The most interesting result obtained from the SANS fits is the systematic decrease in the vesicle core radius from 969.5 ± 17.3 Å in the unconfined case to 446.5 ± 13.4, 106.5 ± 2.0, and 74.8 ± 4.0 Å in the 3300, 550, and 220 Å voids, respectively. This result has important implications for all situations where surfactant aggregate structures are formed in domains where the characteristic dimensions approach the size of the aggregates.

A simple thermodynamic model that captures the essential physics that can predict these changes is described next. In this context, enthalpic (curvature elasticity) contributions to the change in Gibbs free energy arises because of vesicles assuming curvatures that are different from their preferential one, while entropic contributions arise from changes in the free volume fraction. The change in enthalpy, ΔH, per unit void volume is given by[19]

$$\Delta H = \left[\frac{1}{2}\kappa\left(\frac{2}{r} - \frac{2}{r_s}\right)^2 + \bar{\kappa}\left(\frac{1}{r^2}\right)\right](4\pi r^2)\left(\frac{N}{KR^3}\right) \quad (2)$$

Here, κ is the mean bending modulus, $\bar{\kappa}$ is the splay modulus of the vesicle bilayer, r is the radius of vesicle in confinement and, r_s^{-1} is the spontaneous curvature of the vesicle. N is the number of vesicles in a void of volume KR^3, where R is the characteristic dimension of a void and K is a prefactor that depends upon the void geometry (e.g., $K = 8$ for a cubic void and $4\pi/3$ for a spherical void). In the unconfined case (eq 2) leads to the following expression for the equilibrium radius.

$$r_e = \frac{2\kappa + \bar{\kappa}}{2\kappa} r_s \quad (3)$$

Assuming all of the surfactant to be in the form of vesicles, conservation of surfactant mass gives

$$N_e r_e^{\,2} = N r^2 \quad (4)$$

Here, N and r are the number and radius of vesicles present in volume KR^3, and the subscript e denotes the unconfined case. We have assumed a constant area per surfactant headgroup.

In the unconfined case, the contribution to the total excluded volume arises only from the presence of other vesicles. Using a hard sphere model, each vesicle will exclude four times its own volume.[20] Hence, the total free volume fraction can be expressed as

$$\frac{KR^3 - 4\left(\frac{4}{3}\pi r_e^{\,3}\right)N_e}{KR^3} = 1 - 4\left(\frac{4}{3}\pi r_e^{\,3}\right)\left(\frac{N_e}{KR^3}\right) \quad (5)$$

(In eqs 5–8, we have assumed that the vesicle radius is the mean of the inner and outer radii. Thus, the volume of the shell is given by either side of eq 5.) In the confined case, an additional contribution to the free volume fraction comes from the presence of confinement walls, since the vesicles cannot approach the wall closer than a distance equal to their radius r. Therefore the additional excluded volume due to the presence of walls is $KR^3 - K(R-r)^3$. Hence, the total free volume fraction in the confined domains is given by

$$\frac{(KR^3) - [(KR^3) - K(R-r)^3] - 4\left(\frac{4}{3}\pi r^3\right)N}{KR^3} = \frac{(R-r)^3}{R^3} - 4 \times \left(\frac{4}{3}\pi r^3\right)\left(\frac{N}{KR^3}\right) \quad (6)$$

The number of vesicles, N, of radius r in a volume KR^3 is given by

(18) Xia, Y.; Goldmints, I.; Johnson, P. W.; A., H. T.; Bose, A. *Langmuir* **2002**, *18*, 3822–3828.

(19) Helfrich, W. *Z. Naturforsch., C: Biochem., Biophys., Biol., Virol.* **1973**, *28*, 693–703.

(20) Israelachvili, J. N. *Intermolecular and surface forces*; Academic Press: San Diego, CA, 1985.

$$N = \frac{KR^3 V_{fs}}{4\pi r^2 t} \tag{7}$$

where V_{fs} is the volume fraction occupied by the surfactant bilayer and t is the thickness of the bilayer. Similarly, for the unconfined case the number of vesicles N_e in a volume KR^3, can be expressed as

$$N_e = \frac{KR^3 V_{fs}}{4\pi r_e^2 t} \tag{8}$$

The free volume entropy is given by[21]

$$S = kLn(\Omega) \tag{9}$$

where Ω is the free volume fraction. With eqs 5–9, the free volume entropy change, ΔS, going from the unconfined to the confined case can be expressed as

$$\Delta S = \frac{k}{KR^3}\left[Ln\left\{\left(\frac{R-r}{R}\right)^3 - \frac{4V_{fs}r}{3t}\right\} - Ln\left\{1 - \frac{4V_{fs}r_e}{3t}\right\}\right] \tag{10}$$

With eq 2 and eq 10, the change in Gibbs free energy becomes

$$\Delta G = \frac{V_{fs}}{t}\left[2\kappa\left(\frac{1}{r} - \frac{1}{r_s}\right)^2 + \frac{\bar{\kappa}}{r^2}\right] - \frac{kT}{KR^3}\left[Ln\left\{\left(\frac{R-r}{R}\right)^3 - \frac{4V_{fs}r}{3t}\right\} - Ln\left\{1 - \frac{4V_{fs}r_e}{3t}\right\}\right] \tag{11}$$

The change in Gibbs free energy is minimized with respect to the radius of the vesicle by setting $\partial\Delta G/\partial r = 0$. This gives an expression relating the confinement length scale, R, and the vesicle radius, r. The dimensionless form of this equation, obtained by scaling all lengths with r_e and the bending modulus with kT is

$$\frac{4\kappa_1^* V_{fs}}{t^* r^*}\left(\frac{1}{r^*} - 1\right) - \frac{1}{KR^*}\left[\frac{\frac{3(R^* - r^*)^2}{R^*} + \frac{4V_{fs}}{3t^*}}{\left(\frac{R^* - r^*}{R^*}\right)^3 - \frac{4V_{fs}r^*}{3t^*}}\right] = 0 \tag{12}$$

where $\kappa_1 = \kappa + \bar{\kappa}/2$, and $\kappa_1^* = \kappa_1/kT$. Figure 2 is a plot of the dimensionless vesicle radius, $r^* = r/r_e$, versus the dimensionless confinement length scale, $R^* = R/r_e$, for the dimensionless bilayer bending modulus $\kappa_1^* = \kappa_1/kT = 0.15$.[22] The values of geometric prefactor K are taken to be 4 and 20 for this plot, corresponding to a spherical void geometry and a void geometry corresponding to the space between packed spheres,[23] respectively. The dimensionless vesicle wall thickness is taken to be $t^* = 30$ Å/999.5 Å $= 0.03$, and $V_{fs} = 0.0114$ (calculated using the known surfactant weight fraction of 0.8 wt %, an assumed density of the bilayer of 0.77 g/cm^3 corresponding to a 16 carbon aliphatic hydrocarbon liquid and the density of the CM solvent). The equilibrium vesicle size increases with increase in void size and asymptotically tends to the bulk vesicle size as the confinement size increases. The experimental data are also shown on the same plot and show a qualitative match with the predictions from the simple model. The lack of sensitivity to K implies that the equilibrium vesicle size is not controlled by the specific geometry of the voids but rather by its characteristic dimensions.

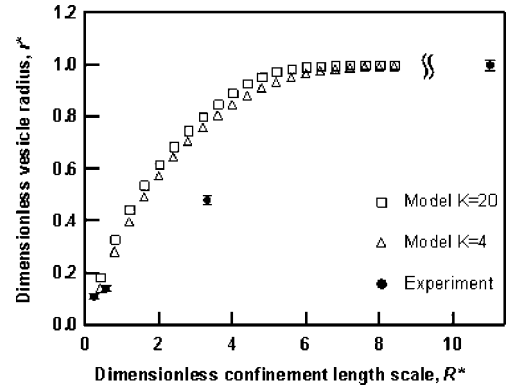

Figure 2. Predictions of vesicle size variation with changes in the length scale of confinement from a simple thermodynamic model. Dimensionless vesicle radius, $r^* = r/r_e$ (r_e is the radius of unconfined vesicles), versus dimensionless confinement radius, $R^* = R/r_e$. The experimental data are also shown.

4. Conclusions

Micellar solutions of CTAB and HDBS are mixed and allowed to self-assemble in an unconfined domain, as well as in void spaces created by the random close packing of polystyrene beads. Vesicles formed when there is no confinement. As the confinement dimensions are decreased, vesicles of lower radius of curvature are formed. A simple thermodynamic model that accounts for changes in enthalpy produced by forming vesicles of radii smaller than the equilbrium one, and changes to the free volume entropy upon confinement show trends that essentially match the experimental data. The essence of the model is that the free volume fraction decreases with increasing confinement. With mass conserved, decreasing the vesicle size allows the free volume fraction to increase and permits an entropic gain that compensates for the enthalpic loss associated with forming vesicles of size away from the equilibrium one.

Acknowledgment. This work is supported by grants from the ACS Petroleum Research Fund to A.T. (44637-G9) and from the NSF to A.B. (CBET 0730392) and by a URI Graduate Fellowship to A.J. We thank B. Hammouda and P. Butler for the extensive support at NIST. We thank N. Balsara, A. Chakraborty, and S. Kline for several important discussions. The SANS instrument at the NIST is supported by the National Science Foundation (DMR-9423101).

Supporting Information Available: Experimental determination and assessment of the bead packing fraction, contrast matching of solvent with polystyrene beads, assessment of the effect of preferential adsorption, effects of using the exact expression and the expression from the thin shell approximation for the vesicle volumes in eqs 5−8 on the final r^* vs R^* curve, and computations accounting for uncertainties in the bead volume fraction and adsorbed layer thickness. This material is available free of charge via the Internet at http://pubs.acs.org.

LA704023S

(21) Helal, K.; Biben, T.; Hansen, J. P. *J. Phys.: Condens. Matter* **1999**, *11*, L51–L58.
(22) Coldren, B.; Zanten, R. v.; Mackel, M. J.; Zasadzinski, J. A.; Jung, H. T. *Langmuir* **2003**, *19*, 5632–5639.
(23) Eriksson, F. *Mathematics Mag.* **1990**, *63*, 184–187.